J|A|C|S
COMMUNICATIONS

Grafting and Coloring onto Silver Nanoparticles by Photoinduced Surface Modification

Hucheng Zhang,* Liwei Zhang, and Jianji Wang

School of Chemistry & Environmental Sciences, Henan Normal University, Xinxiang, Henan 453007, China

Received June 10, 2009; E-mail: hzhang@henannu.edu.cn

Localized surface plasmon resonance (LSPR) is the general optical phenomenon of noble metal nanoparticles.[1] It results from the collective oscillation of conduction electrons and is responsible for the brilliant colors of metal colloidal solutions. The resonance frequency of LSPR can be easily tuned by the size, shape, composition, and microenvironment properties of the nanoparticles,[2−4] and hence noble metal nanoparticles are potentially very useful materials in many application fields, such as optical devices,[5] optical energy conversion,[6] catalysis,[7,8] near field scanning optical microscopy,[9] surface enhanced spectroscopies,[10,11] chemical and biological sensors, etc.[12−14] Especially, the surface modification of noble metal nanoparticles can be easily carried out with alkanethiols, biomolecules, polymers, or other ligands.[15,16] Nanoparticles via surface modifications can create new functional materials and meet the requirements in the applications described above. Therefore, nanoparticles with versatile surface chemistry have been the subject of intensive studies.

Using α-bromoisobutyric acid (BIBA) as the surface modifier, in this work, a new method was developed for the surface modification of silver nanopartiles (Ag NPs). The modified Ag NPs via this method possess several desirable characteristics. The surface chemistry, and also the colors of Ag NPs, can be simply controlled by UV irradiation. The purple Ag NPs have a core/shell nanostructure with a dense encapsulation layer on their surface. This modification not only retains the dispersibility of the Ag NPs in water but also produces nanoparticles with the surface of different chemical components to effectively protect them from deterioration in aqueous media and to be available for further surface modification.

Ag NPs were synthesized via ascorbic acid reduction of silver nitrate using ethanol as solvent in the presence of poly(*N*-vinyl-2-pyrrolidone) (PVP).[17] The ethanol colloidal solution of the Ag NPs (sample 1) appears as dark orange with the extinction maximum at 410 nm (Figure 1). As the ethanol solution of BIBA was injected into sample 1, unexpectedly, no deposition but a pale blue colloidal solution (sample 2) was formed. Under UV irradiation, sample 2 exhibited consecutive color changes and presented blue after 10 h (sample 3), dark blue after 36 h (sample 4), and finally purple after 72 h (sample 5) with the extinction maximum at 531 nm. The red-shift phenomenon can be also observed by controlling the morphology of Ag NPs.[18] Depending on the intended study, any color of Ag NPs in the process can be obtained by removing the sample from UV source. Thereafter, no color change was detected with further radiation for 1 week.

Figure 2 shows the transmission electron microscope (TEM) images of samples at three typical stages of the interface reactions. The Ag NPs in sample 1 have an average size of 26 nm with a standard deviation of 4 nm (26 ± 4 nm). Because of the strong chemisorptions of Ag NPs toward BIBA, however, Ag NPs in sample 2 form spindle-shaped agglomerates 226 ± 31 nm in length and 64 ± 7 nm at maximum diameter. Each agglomerate consists of ∼15−20 Ag NPs. Moreover, it is clearly observed that the Ag NPs in sample 5 possess a core/shell nanostructure and have a size of 41 ± 9 nm with a dense organic shell of ∼8 nm in average thickness. All these experimental results imply that chemical reactions occur on the Ag NP surface.

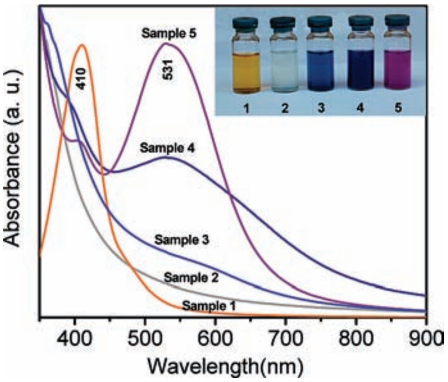

Figure 1. UV−vis spectra of samples at the different reaction stages. Inset shows the photographs 1−5, respectively corresponding to samples 1−5.

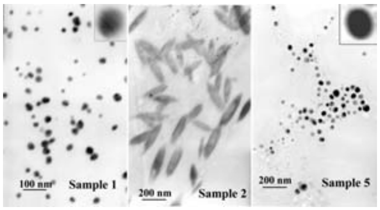

Figure 2. TEM images of the samples. Insets show the images of single nanopartile magnified respectively from samples 1 and 5.

The optical properties of Ag NPs are one of the most interesting aspects. This work shows that the interface reactions can alter the frequency of conduction electron oscillation and, consequently, change the color of Ag NPs. Presumably, the occurrence of strong chemisorptions in sample 2 suppresses the free conduction electrons. When sample 2 is exposed to UV irradiation, the interactions between Br in BIBA and Ag NPs are gradually weakened, and hence the collective oscillation of conduction electrons becomes increasingly significant with the progression of interface reactions. At the same time, Ag NPs are subjected to the varied circumstances of surface chemistry and present themselves in a serial tone in the range of visible spectrum. Obviously, the conversion of molecular kind and composition on the surface of Ag NPs is definitively responsible for the color evolution, and consequently it becomes necessary to reveal the mechanisms of color variations by investigating the chemical reactions on the Ag surface and in the bulk solutions.

The changes of chemical components with the reaction progress in the solutions are revealed by gas chromatography−mass spectrometry (GC−MS) (Scheme 1 and Figures S1−S8). PVP is

10.1021/ja9047416 CCC: $40.75 © 2009 American Chemical Society

Scheme 1. Chemical Changes of α-Bromoisobutyric Acid in the Solutions

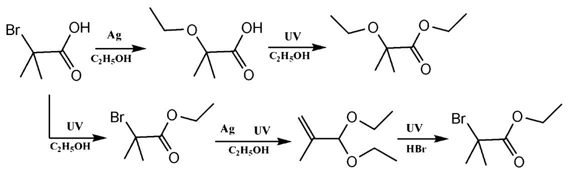

proved to be a useful protecting polymer and has been applied successfully to prepare noble metal nanoparticles in various systems.[19] However, the physical adsorption of Ag NPs is weak toward the solvent-swollen PVP and results in the loose distribution of polymeric segments over nanoparticles.[15] Hence, the strong chemisorptions can still occur between BIBA and Ag NPs in sample 2, and BIBA and α-ethoxyisobutyric acid are determined to be the main components in the solution. This indicates that the interface reactions hardly proceed after the chemisorptions, whereas they can remarkably progress under UV irradiation and cause the change of chemical components in the solutions. At the stage situated by sample 4, the interface reactions have progressed to a great extent, and 2-methyl-3,3-diethoxy-1-propylene is identified as the main component in the solution. The color changes of Ag NPs from pale blue to dark blue are directly related to the extent of interface reactions and, hence, to the chemical components on the surface of Ag NPs. For sample 5, the GC−MS analysis shows that the main component in the solution is ethyl α-bromoisobutyrate (EBIB), and its content is roughly the same as that of the originally added BIBA within experimental error. In the control experiment without Ag NPs, no change is detected in the ethanol solution of PVP and BIBA except that BIBA turns readily into EBIB, confirming the unique role played by Ag NPs in the coloration. From these results, it follows that the coating onto Ag NPs does not result from BIBA but rather from PVP; that is, the PVP segments attached to Ag NPs are responsible for the color changes from dark blue to purple. Presumably, when Br element leaves the Ag NPs, the activated Ag atoms are left behind on the nanoparticle surface. The interactions of ketone groups of PVP with the activated Ag atoms are so strong that PVP segments are grafted on the Ag surface to form the core/shell nanostructure. Figure 3a represents the main components on the surface of Ag NPs in these samples, which can be further confirmed by X-ray photoelectron spectroscopy (XPS) and FT-infrared (FT-IR) spectroscopy.

All samples were respectively deposited on quartz glass to form the films of nanocomposites, and the measurements of XPS and FT-IR were carried out on the solid samples without volatilizable molecules. For sample 2, the Ag 3d and Br 1s peaks in the X-ray photoelectron spectra exhibit the strongest intensity (Figures S9 and S10), indicating that the chemisorptions of Ag NPs to BIBA produce the nearly "naked" naoparticles. Both peaks are still very significant in sample 4. However, they are almost undetected in sample 5, because Br atoms fall away from the surface of Ag NPs and then Ag NPs are densely capped by PVP. Correspondingly, the X-ray photoelectron spectra in O 1s region show three chemical states of oxygen and present the significant changes with the progress of interface reactions (Figure 3b). The shift of O 1s peak of PVP from 530.3 to 529.3 eV gives the indication of interactions of oxygen with Ag NPs in sample 1.[20,21] It is noticed that the relative intensity of the peak at 529.3 eV decreases with the reaction progress and finally disappears in sample 5. Instead, O 1s peak at 531.5 eV is detected in sample 5, which results from the occurrence of C−O as PVP segments are grafted to Ag NPs. In addition, the FT-IR spectrum of sample 1 is similar to that of PVP but is very different from that of sample 5 in the spectral range 1800−1000 cm^{-1} (Figure S11). The peaks at 1175 and 1114 cm^{-1} in the FT-IR spectrum of sample 5 represent the presence of the stretching vibration of C−O[22] and affirm the PVP graft onto Ag NPs and also the formation of the core/shell nanostructure during the interface reactions.

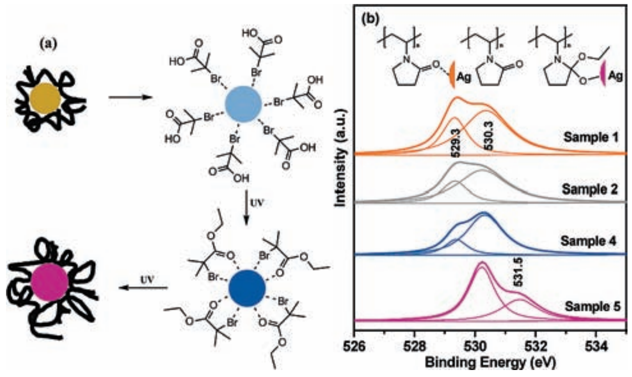

Figure 3. (a) Color change of the Ag nanoparticle with the main component on its surface. (b) Curve fits to the O 1s region of the samples. Inset shows the three chemical states of oxygen in PVP-Ag nanocomposites.

Acknowledgment. The research was supported by the National Natural Science Foundation of China (Grant Nos. 20873036, 20573034) and the Program for New Century Excellent Talents in University of Henan Province.

Supporting Information Available: Full experimental details, GC-MS study, characterization of XPS and FT-IR. This material is available free of charge via the Internet at http://pubs.acs.org.

References

(1) Kreibig, U.; Vollmer, M. *Optical Properties of Metal Clusters*; Springer-Verlag: Heidelberg, Germany, 1995; Vol. 25.
(2) Sun, Y.; Xia, Y. *Analyst* **2003**, *128*, 686–691.
(3) Xue, C.; Mirkin, C. A. *Angew. Chem., Int. Ed.* **2007**, *46*, 2036–2038.
(4) An, J.; Tang, B.; Ning, X.; Zhou, J.; Xu, S.; Zhao, B.; Xu, W.; Corredor, C.; Lombardi, J. R. *J. Phys. Chem. C* **2007**, *111*, 18055–18059.
(5) Zheng, J.; Ding, Y.; Tian, B.; Wang, Z.; Zhuang, X. *J. Am. Chem. Soc.* **2008**, *130*, 10472–10473.
(6) Kamat, P. V. *J. Phys. Chem. C* **2007**, *111*, 2834–2860.
(7) Mitsudome, T.; Arita, S.; Mori, H.; Mizugaki, T.; Jitsukawa, K.; Kaneda, K. *Angew. Chem., Int. Ed.* **2008**, *47*, 7938–7940.
(8) Lu, W.; Gao, S.; Wang, J. *J. Phys. Chem. C* **2008**, *112*, 16792–16800.
(9) Sa´nchez, E. J.; Novotny, L.; Xie, X. S. *Phys. Rev. Lett.* **1999**, *82*, 4014–4017.
(10) Hasell, T.; Lagonigro, L.; Peacock, A. C.; Yoda, S.; Brown, P. D.; Sazio, P. J. A.; Howdle, S. M. *Adv. Funct. Mater.* **2008**, *18*, 1265–1271.
(11) Lu, L.; Kobayashi, A.; Tawa, K.; Ozaki, Y. *Chem. Mater.* **2006**, *18*, 4894–4901.
(12) Elghanian, R; Storhoff, J. J.; Mucic, R. C.; Letsinger, R. L.; Mirkin, C. A. *Science* **1997**, *277*, 1078–1081.
(13) Krämer, S.; Xie, H.; Gaff, J.; Williamson, J. R.; Tkachenko, A. G.; Nouri, N.; Feldheim, D. A.; Feldheim, D. L. *J. Am. Chem. Soc.* **2004**, *126*, 5388–5395.
(14) West, J. L.; Halas, N. J. *Annu. Rev. Biomed. Eng.* **2003**, *5*, 285–292.
(15) Quaroni, L.; Chumanov, G. *J. Am. Chem. Soc.* **1999**, *121*, 10642–10643.
(16) Xue, C.; Li, Z.; Mirkin, C. A. *Small* **2005**, *1*, 513–516.
(17) Sun, Y.; Wiley, B.; Li, Z; Xia, Y. *J. Am. Chem. Soc.* **2004**, *126*, 9399–9406.
(18) Cao, Z.; Fu, H.; Kang, L.; Huang, L.; Zhai, T.; Ma, Y.; Yao, J. *J. Mater. Chem.* **2008**, *18*, 2673–2678.
(19) Washio, I.; Xiong, Y.; Yin, Y.; Xia, Y. *Adv. Mater.* **2006**, *18*, 1745–1749.
(20) Lu, W.; Liu, G.; Gao, S.; Xing, S.; Wang, J. *Nanotechnology* **2008**, *19*, 445711–445720.
(21) Huang, H. H.; Ni, X. P.; Loy, G. L.; Chew, C. H.; Tan, K. L.; Loh, F. C.; Deng, J. F.; Xu, G. Q. *Langmuir* **1996**, *12*, 909–912.
(22) Zhang, H.; Wang, J.; Zheng, H.; Zhuo, K.; Zhao, Y. *J. Phys. Chem. B* **2005**, *109*, 2610–2616.

JA9047416